JOURNAL OF AIRCRAFT
Vol. 44, No. 6, November–December 2007

Aerodynamic Control Using Windward-Surface Plasma Actuators on a Separation Ramp

Javier Lopera* and T. Terry Ng†
University of Toledo, Toledo, Ohio 43606
Mehul P. Patel,‡ Srikanth Vasudevan,§ and Ed Santavicca¶
Orbital Research Inc., Cleveland, Ohio 44103
and
Thomas C. Corke**
University of Notre Dame, Notre Dame, Indiana 46556

DOI: 10.2514/1.30741

Wind-tunnel experiments were conducted on a 47-deg sweep, scaled 1303 unmanned air vehicle model to assess the performance of an innovative windward-surface plasma actuator design for flight control at low angles of attack. Control was implemented by altering the flow past an aft separation ramp on the windward side using a single dielectric barrier discharge plasma actuator. The influence of ramp-expansion angles (20, 30, and 40 deg) on the plasma actuator's ability to affect flow separation and aerodynamic lift was examined. Both steady and unsteady actuations of the plasma actuator were examined, and their effects were captured using lift measurements and flow visualizations. Results reveal that the plasma actuator effects are highly dependent on the ramp angle and actuator parameters such as duty cycle and modulation frequency. The actuators produced significant shifts in the lift curve, up to 25% for the most effective ramp angles of 20 and 30 deg, in the 0–20-deg α range. Flow visualization results confirmed that the plasma actuator causes the flow to reattach over a region downstream of the separation ramp. For all ramp cases examined, the unsteady (pulsed) actuator was more effective than the steady actuator in controlling flow separation and influencing the aerodynamic lift. The aerodynamic effect of plasma actuators was found to be highly dependent on the ramp angle and the separation strength over the ramp. Significant control forces were obtained using windward-surface plasma actuators and, indirectly, these control forces can be implemented to generate substantial control moments for maneuvering air vehicles.

Nomenclature

α	=	angle of attack, deg
C_L	=	lift coefficient
c	=	wing chord
F^+	=	nondimensional frequency of actuator
f_{mod}	=	frequency of modulation, Hz
I	=	current, A
L_{sep}	=	streamwise extent of the separation zone, m
P	=	power, W
Re_c	=	chord Reynolds number
St	=	Strouhal number
U	=	freestream velocity, m/s
V	=	voltage, V
θ	=	phase angle between current and voltage in an ac circuit, rad

Presented as Paper 0636 at the 45th AIAA Aerospace Sciences Meeting and Exhibit, Reno, NV, 8–11 January 2007; received 28 February 2007; revision received 26 March 2007; accepted for publication 1 April 2007.

*Graduate Research Assistant, Department of Mechanical, Industrial and Manufacturing Engineering. Member AIAA.
†Professor, Department of Mechanical, Industrial and Manufacturing Engineering. Senior Member AIAA.
‡Director, Aerodynamics Group. Senior Member AIAA.
§Aerospace Engineer. Member AIAA.
¶Engineering Specialist.
**Clark Chair Professor, Aerospace and Mechanical Engineering Department, Associate Fellow AIAA.

I. Introduction

THERE has been an increased interest in recent years in expanding the functions of unmanned air vehicles (UAVs) for both civilian and military operations. Technologies that enable revolutionary capabilities in augmenting the performance of UAVs are being developed worldwide. One such technology is active flow control (AFC). AFC offers methodologies that can expand the flight envelope of UAVs, improve their aerostructural performance, and also free up the design space from the constraints of traditional aerodynamic control systems. This paper discusses an innovative active flow control approach involving a windward-surface single dielectric barrier discharge (SDBD) plasma actuator as a flow control device for providing lift and pitch control on a 1303 UAV configuration. Earlier work by Patel et al. [1] focused on lift enhancement at high angles of attack through leading-edge vortex control using plasma actuators. The present study investigates lift control at low angles of attack using a plasma actuator at the lip of a backward-facing separation ramp on the windward surface near the trailing edge. This paper presents experimental evidence of the control effectiveness of a windward-ramp plasma flow control concept at a flow Reynolds number of $Re_c = 4.33 \times 10^5$.

The alternating current (ac) glow discharge SDBD plasma actuator offers tremendous potential as a flow control device because of its simple lightweight design with no moving parts and low power consumption. It has been shown to provide good control effects at low speeds. In recent years, there have been numerous demonstrations on the use of a SDBD plasma actuator for controlling fluid flows. Examples include exciting boundary-layer instability modes on a sharp cone at Mach 3.5 by Corke et al. [2], boundary-layer control by Roth et al. [3], lift augmentation on a wing section by Corke et al. [4], separation control on a high-angle-of-attack airfoil using plasma actuators by Post and Corke [5], separation control on stationary and oscillating airfoils by Post and Corke [6], plasma flaps and slats for hingeless flight control by Corke et al. [7], boundary-layer flow control by Jacob et al. [8], smart

plasma slats for autonomous sensing and control of wing stall by Patel et al. [9], plasma optimized airfoil by Corke et al. [10], and plasma wings for hingeless flight control of a UAV by Patel et al. [1]. A more detailed background on the physics and behavior of plasma actuators are provided by Enloe et al. [11,12], and an overview of some of the recent developments of the SDBD actuator are presented by Corke et al. [13].

A majority of past work on the use of a plasma actuator as a flow control device has focused on flat-plate and two-dimensional geometries. A recent study by Patel et al. [1] has shown experimental evidence on the use of a plasma actuator for flight control of a three-dimensional geometry: a 47-deg-sweep 1303 UAV. Although the control demonstration was good at high angles of attack (between $\alpha = 15$ and 25 deg), no effects were produced at low angles of attack ($\alpha < 14$ deg). Results from a flow visualization study conducted on the 1303 UAV model suggest that at below $\alpha \sim 15$ deg, the leading-edge vortices are intact and thus too strong to be affected by plasma. Above $\alpha \sim 15$ deg, the vortices break down and so the leeward flow is essentially that of a stalled wing, which enables the effect of plasma to be more pronounced.

Additionally, results from flow visualization experiments conducted in a water tunnel revealed that the windward surface (pressure side) provided a relatively simpler (two-dimensional) flow structure that is fully attached [1]. There appears to be little, if any, crossflow component on the windward surface of the wing section. This is in strong contrast to the leeside (suction side) flow, which exhibited a strong crossflow component. These results suggest that the windward-side (pressure-side) flow is potentially more receptive to control than the suction side.

Because of the predominant complex 3-D flow structure on the suction side, which is difficult to control, and the simpler 2-D flow structure on the pressure side, seemingly controllable via simple plasma actuator geometries, the current study was undertaken to investigate the effect of a novel windward-ramp plasma flow control concept for achieving lift control at low angles of attack. The purpose of the present work is to investigate the behavior of steady and unsteady plasma-induced flow over different separation-ramp angles on the windward surface for lift control. The concept of manipulating the flow past a separation ramp to influence the aerodynamic performance of a control surface using a flow control device is not new; however, the application of this technique on the windward surface to achieve lift control has not been examined before.

The main objectives of the present work were to 1) assess the performance of plasma actuators in conjunction with a windward separation ramp for providing lift control at low angles of attack and 2) improve the control effectiveness by optimizing the backward ramp angle and actuator parameters such as unsteady (modulation) frequency and duty cycle.

II. Experimental Setup

A. UAV Test Model

The design of the 1303 UAV test model is described in detail in the paper by Patel et al. [1]. The UAV model has a leading-edge sweep of 47 deg with varying cross sections and a trailing-edge sweep of ± 30 deg, as shown in Fig. 1. The present experiments were conducted on a 4.16%-scale half-span UAV model with a 0.4-m root chord and 0.34-m span. Wind-tunnel experiments were conducted at the University of Toledo's low-speed closed-return wind tunnel with a 0.9×0.9 m (3×3 ft) test section. Experiments were conducted at a chord Reynolds number of 4.33×10^5, based on the mean chord c of 0.2 m and freestream velocity of 15 m/s for angles of attack ranging from -10 to 26 deg at 2-deg increments.

A force balance mounted on top of the wind-tunnel ceiling was used for the present experiments. The wing model was connected to a high-precision 495-Series 3-in. rotary stage that was controlled using a Newport 855C programmable controller and a remote controller for model positioning. Using this system, the measurement accuracy of the angle of attack was ± 0.001 deg. A schematic of the experimental setup is shown in Fig. 2.

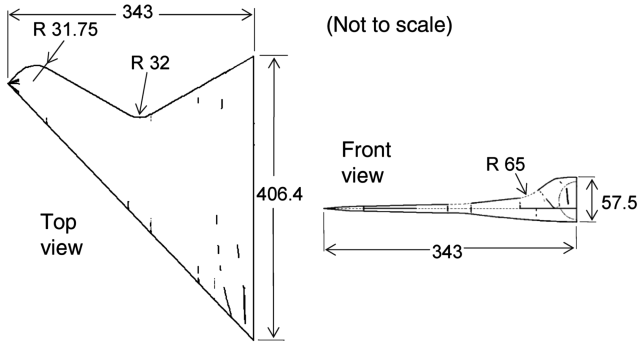

Fig. 1 Schematic of the UAV wing tested. Dimensions are in millimeters.

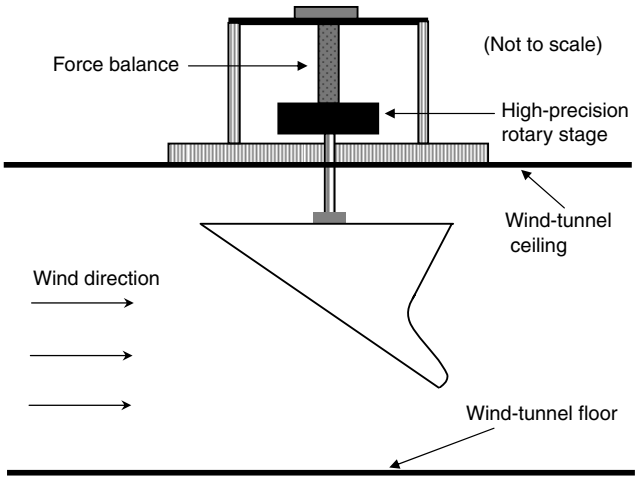

Fig. 2 Wind-tunnel experimental setup.

Two tempered-glass sidewalls and a large Plexiglas window on the ceiling provided convenient access for flow visualization from different viewing angles. The flow in the test section was uniform, with a turbulence level of less than 0.2% outside of the wall boundary layers.

For every angle of attack, 30,000 samples were taken at a sampling rate of 2000 samples per second. Initial tests were composed of one data sample, and later, three data samples were collected and ensemble-averaged for each test case. Lift forces were measured, and the accuracy of lift data was verified by repeat measurements. The average standard deviation in the lift coefficient was 0.00496.

B. Plasma Actuators

The SDBD plasma actuator configuration consists of two electrodes that are separated by a dielectric material. One of the electrodes is usually exposed to the surrounding air and the other is fully encapsulated by a dielectric material. When a large ac potential, hereafter referred to as *ac carrier frequency*, is applied to the electrodes at sufficiently high amplitude levels, the air in the region of the largest potential ionizes and plasma is produced. The ionization typically occurs at the edge of the electrode that is exposed to the air and spreads out over the area projected by the covered electrode, directing momentum into the surrounding air.

In the present study, two strips of plasma actuators were placed immediately upstream of the separation ramp: one in the inboard section and the other in the outboard section. The actuators were fabricated using two 0.05-mm-thick copper electrodes, which were separated by two layers of 0.1-mm-thick Kapton film. Both inboard and outboard actuators were operated in a similar configuration. The electrodes were arranged in an asymmetric configuration, as shown in Fig. 3. The two electrodes were overlapped by a small amount, approximately 1 mm, to ensure uniform plasma was formed in the

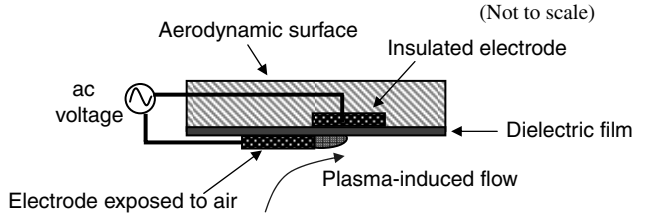

Fig. 3 Schematic for windward-side aerodynamic plasma actuator; configuration shown is composed of two electrodes arranged asymmetrically between a Kapton (dielectric) film.

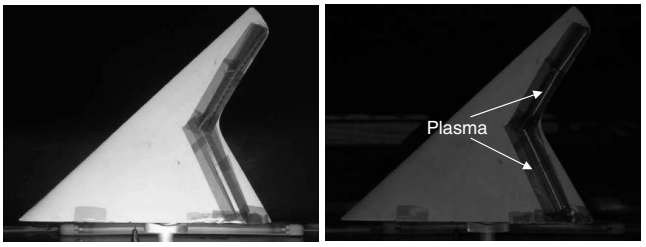

Fig. 4 Pictures of aerodynamic plasma actuators mounted at the onset of the separation ramp on the windward surface near the trailing edge; (left) baseline configuration (plasma off) and (right) plasma actuator on.

spanwise direction. The plasma actuator was bonded to the surface using a foil tape that was attached to the base of the electrodes. The two copper-foil electrodes were aligned in the spanwise direction and mounted at the reflex line of the separation ramp.

The amount of power applied to a plasma actuator is determined using the formula $P = (I \times V) \times \text{cosine}(\theta)$. The phase angle on a typical transformer/actuator assembly can be as high as 70 deg. Any phase shift between the voltage and current reduces the system efficiency and may also cause instability in the power amplifier. With a phase shift of 70 deg, the system efficiency is only 34%, implying that 66% of the power is dissipated in the form of heat. For the current experiments, a phase-angle detector was custom-made to obtain the optimum ac carrier frequency and increase the effectiveness and efficiency of the SDBD plasma actuators in producing control forces on a UAV configuration.

The actuators were tested in both unsteady and steady modes of operation for different duty cycles. For unsteady tests, the actuators were operated at $F^+ = 1$, based on the Strouhal number scaling $St = F^+ = (f_{\text{mod}} \times L_{\text{sep}})/U = 1$. This yielded a modulation frequency $f_{\text{mod}} = 395$ Hz, based on the average length of L_{sep} and the selected air speed. The duty cycle is the percentage of time in a period that the actuator is on; thereby, a steady actuator operates at a 100% duty cycle. Figure 4 shows a photograph of the plasma actuators mounted at the onset (reflex line) of the separation ramp on the windward surface of the wing.

C. Separation Ramp

The UAV test model was modified on the windward surface to incorporate a backward-facing separation ramp near the trailing edge. The basic premise for incorporating a ramp is to induce flow separation past the ramp at low to moderate angles of attack. This region of separated flow aft of the ramp can subsequently be influenced by a plasma actuator to cause a shift in the lift characteristics of the wing. Initial tests of the control concept using flow visualizations with tufts for plasma on and off conditions revealed a strong dependency on the actuator effects on the ramp-divergence angles, which, in fact, control the "degree" of flow separation over the ramp. Therefore, several backward ramp angles (20, 30, and 40 deg) were studied with plasma on and off to determine an optimal setting for maximum effect on lift. Figure 5 shows a schematic of the UAV with different ramp angle settings. Figures 6 and 7 show pictures of the modified UAV design with a 20-deg

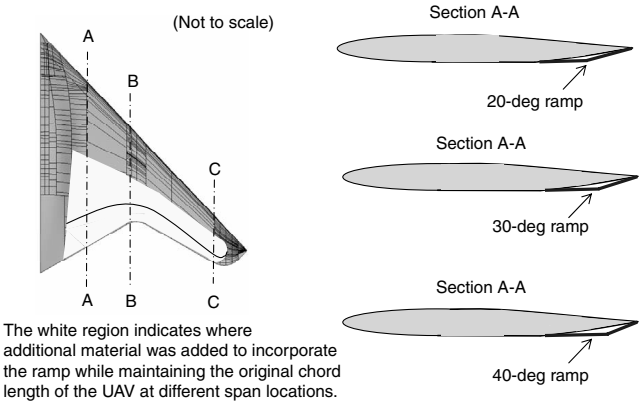

Fig. 5 Schematic of a modified UAV wing tested for different expansion-ramp angles near the trailing edge of the windward surface.

Fig. 6 Picture of the modified wing model; (left) leeward surface and (right) windward surface.

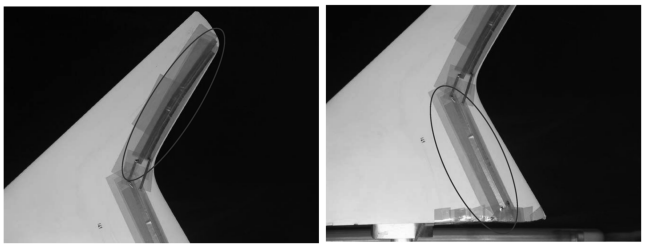

Fig. 7 Picture of aerodynamic plasma actuators mounted at the onset of the 20-deg separation ramp on the windward surface; (left) outboard region plasma actuator and (right) inboard region plasma actuator.

separation ramp near the trailing edge of the windward surface. Two strips of SDBD plasma actuators were mounted at the onset of the separation ramp: one on the inboard section and the second on the outboard section of the wing.

III. Results

Results are presented in the form of measured lift coefficient and flow visualizations records using tufts with the plasma actuator on and off. The aerodynamic effect of the windward-surface plasma actuators are assessed by examining the change in the lift coefficient for baseline configurations (plasma off) and control configurations (plasma on). For flow visualization results, plasma-induced changes in the baseline flow are examined using tufts mounted on the wing surface to determine the separated/attached state of the flow as it passes over the ramp.

A. Force Measurements

1. *Comparison of Aerodynamic Performance of Modified UAV Designs*

For a practical implementation of a flow control technique on an air vehicle, in addition to producing significant control forces/moments for flight control, it is also imperative that is does not compromise the aerodynamic performance of the vehicle in its

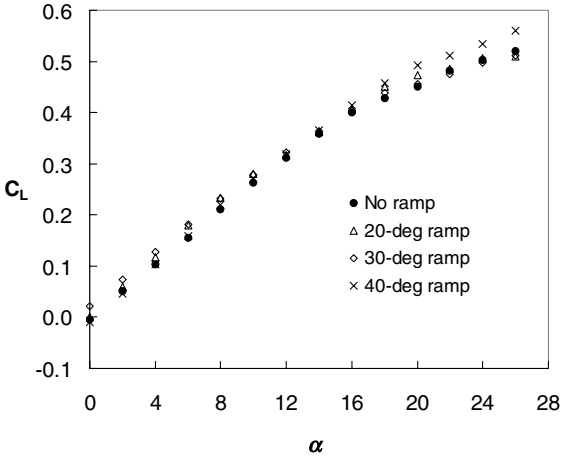

Fig. 8 Comparison of the effect of windward-surface backward ramp angles on the coefficient of lift vs angle of attack for baseline (control off) configurations.

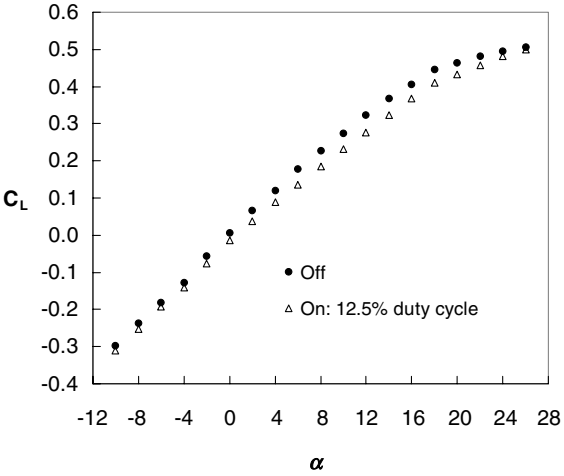

Fig. 9 Coefficient of lift vs angle of attack; plasma actuators pulsed with a 12.5% duty cycle, $F^+ = 1$, and $f_{\text{mod}} = 395$ Hz; 20-deg windward-surface separation ramp.

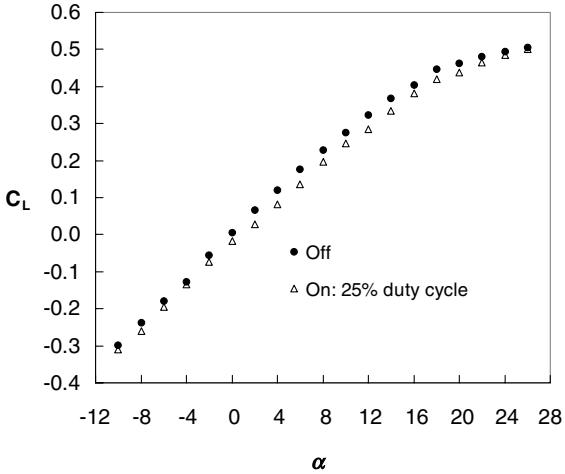

Fig. 10 Coefficient of lift vs angle of attack; plasma actuators pulsed with a 25% duty cycle, $F^+ = 1$, $f_{\text{mod}} = 395$ Hz; 20-deg windward-surface separation ramp.

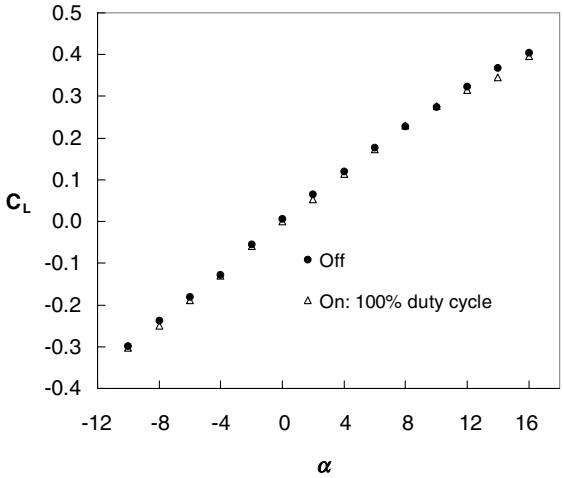

Fig. 11 Coefficient of lift vs angle of attack; plasma actuators pulsed with a 100% duty cycle (steady); 20-deg windward-surface separation ramp.

baseline (actuator off) configuration. In our study, we conducted experiments to compare the effect of different windward-surface separation-ramp angles, including a baseline (no ramp) case, to assess the aerodynamic performance of the air vehicle under different windward configurations. Results in Fig. 8 show that, overall, the use of a windward-surface separation ramp does not have a detrimental effect on the baseline lift coefficient. Results show that the separation ramp leads to a slight increase in the lift coefficient at lower angles of attack. For higher angles of attack, $\alpha > 16$ deg, results show that the 40-deg ramp results in a considerable increase in the lift coefficient when compared with the baseline design. Drag measurements showed small difference in the drag coefficient at low angles of attack (which is the flight envelope for the UAV design examined) for the baseline (no ramp) case and the modified UAV designs with different windward-surface separation-ramp angles.

2. *Effects of Ramp Angle and Duty Cycle*

The first separation-ramp angle tested was a 20-deg windward-surface ramp near the trailing edge. Figure 9 shows the lift coefficient for a baseline case (actuator off) and a controlled case (actuator on), with the plasma actuators operating in an unsteady mode at a 12.5% duty cycle. Results show that the plasma actuators produced a consistent shift in the C_L–α curve for all angles of attack from $\alpha = -2$ to 22 deg. The effect of the windward-surface plasma actuator is a decrease in the C_L, ranging from 6 to 25% from $\alpha = 2$ to 20 deg.

Figure 10 shows results for a case when the plasma actuators were pulsed at a 25% duty cycle. Similar reductions in the lift coefficient were observed for $\alpha = -2$ to 20 deg. In this case, the most significant changes were observed from $\alpha = 2$ to 18 deg, with a decrease in the lift coefficient ranging from 5 to 30%.

Figure 11 shows results from a test conducted with a steady plasma actuator. Results show that a steady plasma actuator has a negligible effect on the lift coefficient. These results demonstrate that a pulsed (unsteady) actuator has a stronger effect on the flowfield than a steady actuator. It has been conjectured that an unsteady actuator produces a series of vortices convecting downstream. When the pulse frequency produces a sufficient number of stable vortices over the surface continuously, flow reattachment occurs. This finding led us to conduct only unsteady plasma actuation experiments for the subsequent investigations (30- and 40-deg ramps). Subsequent studies showed that the most significant control, measured by a decrease in C_L, was achieved by operating the unsteady plasma actuators at a duty cycle of 12.5%. Additional tests were conducted to verify this effect of the unsteady plasma actuators at a 12.5% duty cycle by ensemble averaging three data sets.

Lift coefficients for the three separate tests were ensemble-averaged for the baseline and controlled cases and are presented in Fig. 12. Noticeable reductions in the lift coefficient are observed for $\alpha = 0$ to 20 deg. Results show that the plasma actuator decreases the lift coefficient by 4.8 to 25% for $\alpha = 4$ to 20 deg. These results validate the use of a plasma actuator mounted at the onset of a

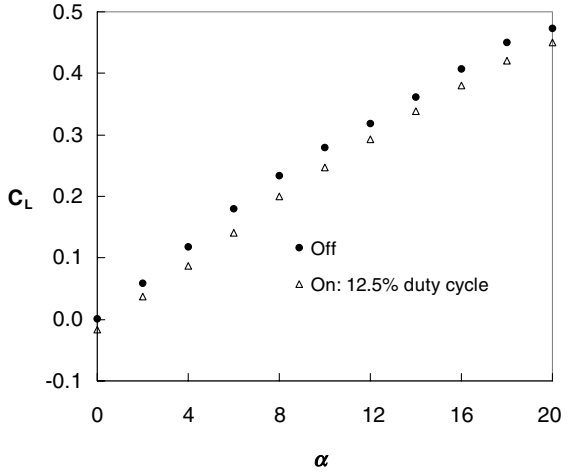

Fig. 12 Coefficient of lift vs angle of attack; ensemble average of three separate tests; plasma actuators pulsed with a 12.5% duty cycle, $F^+ = 1$, and $f_{mod} = 395$ Hz; 20-deg windward-surface separation ramp.

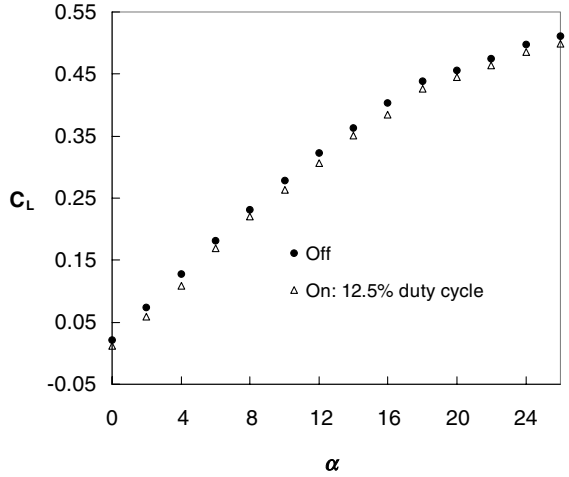

Fig. 13 Coefficient of lift vs angle of attack; plasma actuators pulsed with a 12.5% duty cycle, $F^+ = 1$, and $f_{mod} = 395$ Hz. 30-deg windward-surface separation ramp.

separation ramp near the trailing edge of the windward surface as an effective AFC actuator capable of generating significant control forces.

The next set of tests examined the control on a 30-deg windward-surface separation ramp. Figure 13 shows results for a 12.5% duty cycle plasma actuator mounted at the onset of a 30-deg windward-surface separation ramp. The effect of the controlled case (plasma on) is to decrease the lift coefficient. The plasma actuator decreases the lift coefficient by 2 to 15% over the α range tested, compared with the baseline case. Results for a plasma actuator pulsed with a 25% duty cycle are shown in Fig. 14. The plasma actuator is more effective at a 25% duty cycle on the 30-deg separation ramp. The plasma actuator reduces the lift coefficient by 5 to 17% for the α range tested. The separation over a 30-deg ramp is stronger than the separation observed over a 20-deg ramp. This stronger separation and increased adverse pressure gradient might explain the increased effectiveness of a longer duty cycle (25%) over a shorter (12.5%) duty cycle for the 30-deg separation ramp.

Results for a 40-deg windward-surface separation ramp are shown in Figs. 15 and 16. Overall, the effect of the plasma actuators is reduced at this ramp angle. Results for a 12.5% duty cycle, shown in Fig. 15, show a decrease of 1 to 2% in the lift coefficient for $\alpha > 14$ deg. A similar trend is observed with a 25% duty cycle, shown in Fig. 16, in which the plasma actuator produces a decrease of 1.5 to 3% in the lift coefficient for $\alpha > 16$ deg. It is expected that a

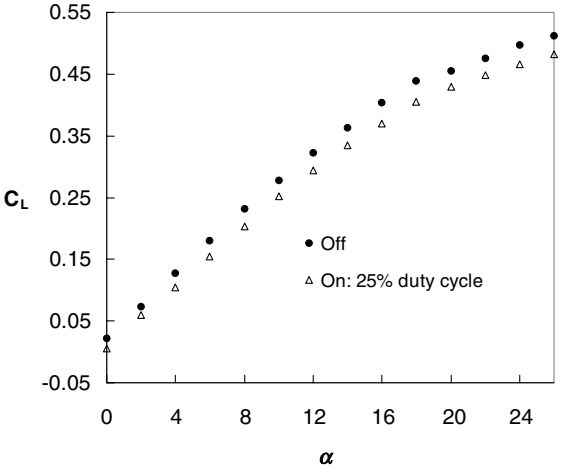

Fig. 14 Coefficient of lift vs angle of attack; plasma actuators pulsed with a 25% duty cycle, $F^+ = 1$, and $f_{mod} = 395$ Hz; 30-deg windward-surface separation ramp.

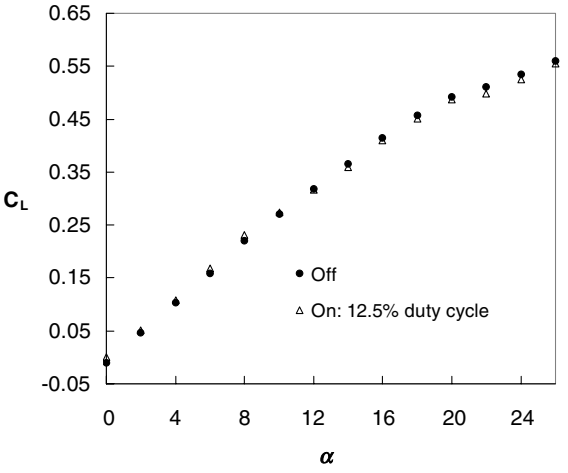

Fig. 15 Coefficient of lift vs angle of attack; plasma actuators pulsed with a 12.5% duty cycle, $F^+ = 1$, and $f_{mod} = 395$ Hz; 40-deg windward-surface separation ramp.

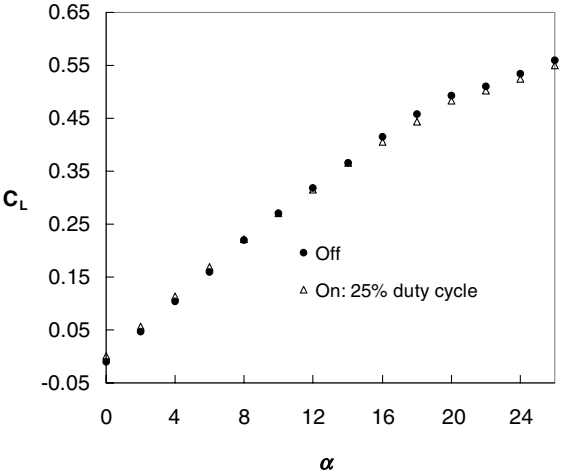

Fig. 16 Coefficient of lift vs angle of attack; plasma actuators pulsed with a 25% duty cycle, $F^+ = 1$, and $f_{mod} = 395$ Hz; 40-deg windward-surface separation ramp.

40-deg ramp will produce a strong separation; thus, the effect of the plasma actuator might not be strong enough to overcome the accompanying strong adverse pressure gradient.

B. Flow Visualization Investigations

Flow visualization studies were conducted to corroborate the force balance data and to gain additional insights into the flow physics associated with the use of a SDBD plasma actuator at the onset of a windward-surface separation ramp near the trailing edge. Flow visualizations were performed by placing arrays of tufts over the plasma actuator and onto the separation ramp. Flow visualizations were captured via a video camera, and the videos were later edited to extract snapshot images of the baseline and controlled cases. The videos were captured at the standard 30 frames-per-second rate. The camera was placed outside of the tunnel for side views of the wing and inside the tunnel for in-plane views of the separation ramp and the aerodynamic plasma actuator. Flow visualization studies were conducted at flow conditions similar to the force measurements. The actuator was operated in an unsteady mode at a duty cycle of 12.5%.

Figs. 17 and 18 show side-view visualizations of the inboard plasma actuator at $\alpha = 6$ and 14 deg, respectively. The sequence of pictures shows that for the baseline case, the flow separates near the onset of the separation ramp. The tufts are observed to be lifted *off* the surface, which indicate a separated flowfield. When the plasma actuator is in operation, the tufts move very close to the wing surface. The movement of the tufts toward the surface is indicative of a reattachment of the flow close to the trailing-edge region. Figure 18 clearly shows the effect of the plasma actuator on the flow past the separation ramp at $\alpha = 14$ deg. The baseline flow separates from the surface as it passes the separation ramp, and the pulsing of the plasma actuator causes the tufts (i.e., the flow) to reattach to the surface.

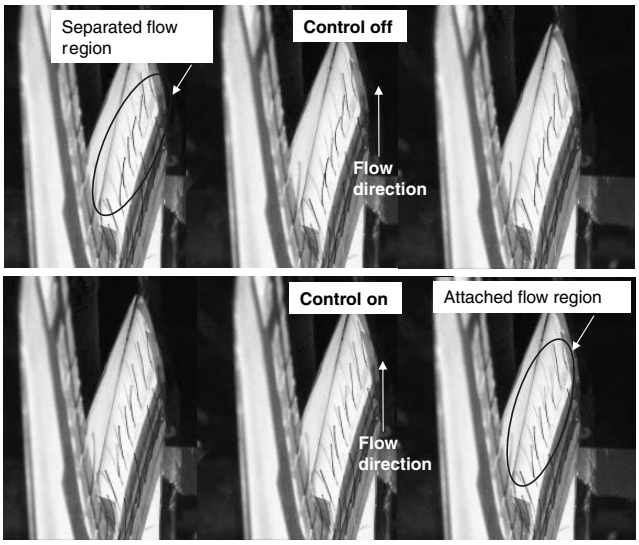

Fig. 17 Side-view sequence visualizations of inboard plasma actuator mounted at the onset of windward-surface 20-deg separation ramp; plasma actuators pulsed with a 12.5% duty cycle, $F^+ = 1$, $f_{\text{mod}} = 395$ Hz, and $\alpha = 6$-deg; (top) control off and (bottom) control on.

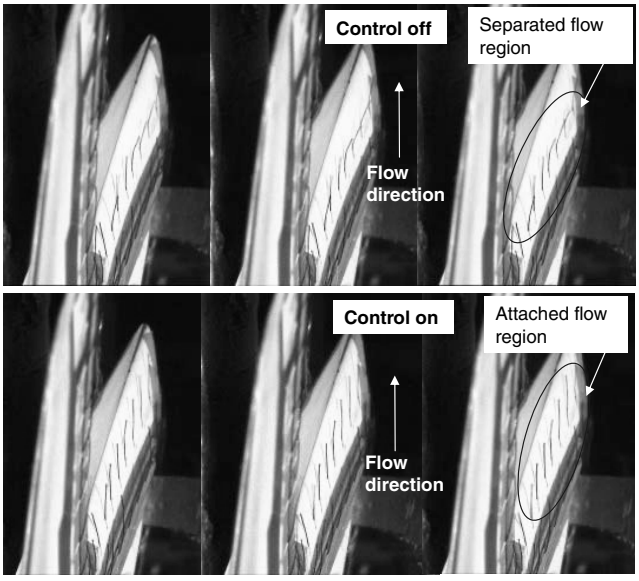

Fig. 18 Side-view sequence visualizations of inboard plasma actuator mounted at the onset of the windward-surface 20-deg separation ramp; plasma actuators pulsed with a 12.5% duty cycle, $F^+ = 1$, $f_{\text{mod}} = 395$ Hz, and $\alpha = 14$-deg; (top) control off and (bottom) control on.

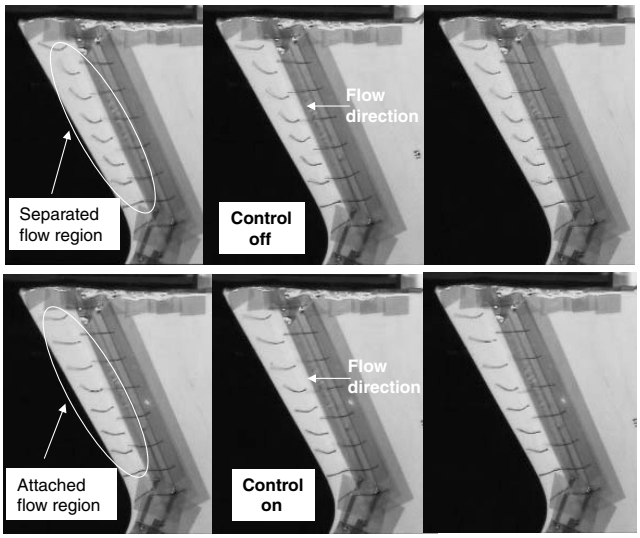

Fig. 19 Planform-view sequence visualizations of inboard plasma actuator mounted at the onset of the windward-surface 20-deg separation ramp; plasma actuators pulsed with a 12.5% duty cycle, $F^+ = 1$, $f_{\text{mod}} = 395$ Hz, and $\alpha = 8$-deg; (top) control off and (bottom) control on.

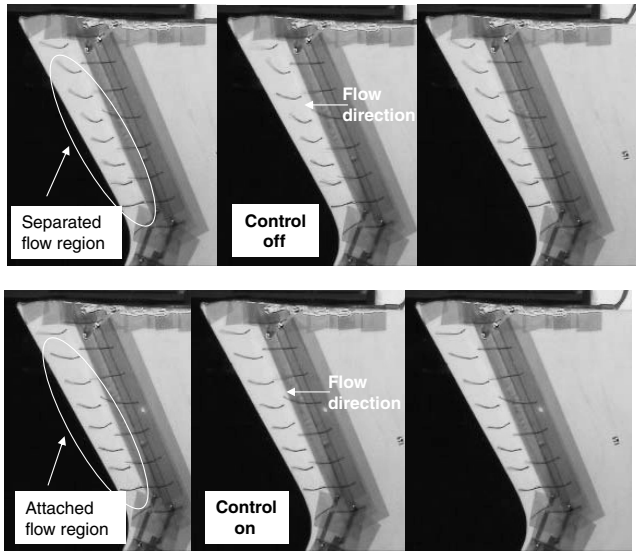

Fig. 20 Planform-view sequence visualizations of inboard plasma actuator mounted at the onset of the windward-surface 20-deg separation ramp; plasma actuators pulsed with a 12.5% duty cycle, $F^+ = 1$, $f_{\text{mod}} = 395$ Hz, and $\alpha = 14$-deg; (top) control off and (bottom) control on.

Planform-view visualizations near the inboard plasma actuator are presented in Figs. 19 and 20 for $\alpha = 8$ and 14 deg, respectively. These images illustrate the flow reversal and separation region that occur past the separation ramp. The tufts past the ramp are observed to be significantly unsteady and oscillate in a direction opposite to the flow, which is indicative of a region of flow reversal. As the plasma actuator is pulsed, the tufts past the ramp are observed to become mostly parallel to the flow, and there is a remarkable reduction in the unsteadiness and oscillations of the tufts. The region of "steady" tufts close to the surface indicates that the flow is mostly attached in the region past the separation ramp.

By examining the flow over the windward surface, the effect of the plasma actuator on the lift coefficient can be assessed. The plasma actuator has the effect of reattaching the flow for some distance downstream of the reflex line of the separation ramp. For the flow to be reattached, the flow close to the reflex line of the separation ramp needs to accelerate around the ramp and a local low pressure is expected to occur. This induced low-pressure region near the windward-surface separation ramp will cause a reduction in the net pressure difference over the wing, and as a result, a decrease in lift is expected. In addition, if the flow is reattached for most of the region aft of the ramp, the effect of the plasma actuator would be to reduce the effective camber of the wings, thereby decreasing the overall lift. Because flow visualizations demonstrate that the plasma actuator reattaches the flow over a region past the reflex line of the separation ramp, the results correlate well with force measurements that show a decrease in the lift coefficient.

IV. Conclusions

Wind-tunnel experiments were conducted to investigate the aerodynamic effect of plasma actuators mounted at the onset of a windward-surface separation ramp near the trailing edge of a 1303 47-deg sweep UAV model. Results presented are proof-of-concept investigations on the use of the technique for aerodynamic control of an air vehicle. Force measurements show that the plasma actuator has the effect of decreasing the lift coefficient compared with the baseline (control off) case. Results also show that an unsteady (pulsed) plasma actuator has a significant effect on the lift coefficient, whereas a steady actuator (100% duty cycle) has a negligible effect.

Three windward-surface separation ramps with backward ramp angles of 20, 30, and 40 deg were examined. Significant reductions in the lift coefficient were obtained using the 20- and 30-deg ramp configurations. For some conditions, reductions of 15 to 25% in the lift coefficient were obtained. With ramp angles higher than 20 deg, a duty cycle of 25% yielded the most significant decreases in the lift coefficient, whereas a 12.5% duty cycle produces the best results for a 20-deg ramp. Further experiments need to be performed to verify the optimal actuator parameters at higher ramp angles.

The ramp angle was found to be a critical design parameter for determining the effectiveness of windward-surface plasma actuators. As the ramp angle increases, the associated adverse pressure gradient past the ramp increases accordingly. At large ramp angles, up to 40 deg in the current study, a large adverse pressure gradient and strong separation overwhelm the actuator effect on the flowfield and render the plasma actuator ineffective.

Flow visualizations for the baseline case showed that the flow separated past the separation ramp and there was a region of flow reversal. In contrast, visualizations of pulsed plasma actuators showed that a region of the flow past the separation ramp was reattached. The partial/complete reattachment of the flow past the ramp is conjectured to produce a low-pressure region around the ramp and thus a decrease in lift. In addition, if the flow is attached aft of the ramp up to the trailing edge, the windward-surface plasma actuator will have the effect of reducing the effective camber of the wing and inducing a reduction in the lift coefficient.

The effect of windward-surface plasma actuators was examined herein at 15 m/s (29 kt). A recent investigation by Patel et al. [14] investigated the scalability and effectiveness of leading-edge separation control on airfoils using SDBD plasma actuators. Their experiments demonstrated that the SDBD plasma actuator was effective in reattaching the flow for chord Reynolds numbers up to 1.0×10^6 and freestream speeds up to 60 m/s (117 kt). They also showed that the optimum unsteady actuator frequency f_{mod} minimized the actuator voltage needed to reattach the flow, such that $F^+ = (f_{\text{mod}} \times L_{\text{sep}})/U = 1$. In addition, Patel et al. indicated that at the optimum frequencies, the minimum voltage required to reattach the flow was weakly dependent on the chord Reynolds number and strongly dependent on the poststall angle of attack and leading-edge radius.

Although moment measurements were not directly measured, it can be indirectly inferred from the reduction of the local lift coefficient that rolling and pitching moments could be generated by placing the control at different parts of the air vehicle. These induced moments can potentially be used to control and alter the dynamics of the air vehicle. The flow over the windward surface of different wing planforms is expected to resemble a 2-D flow with a weak or negligible crossflow component. These characteristics of the windward flow make the windward surface a very attractive location to successfully implement plasma actuators for aerodynamic control of many different air vehicles.

Acknowledgments

This work was supported by Orbital Research, Inc., under a Small Business Innovation Research Phase II Contract No. FA8650-04-C-3405 issued by the U.S. Air Force Research Laboratory (AFRL). The authors would like to thank Charles F. Suchomel, AFRL Program Monitor, for his insightful remarks and support of this work.

References

[1] Patel, M. P., Ng, T. T., Vasudevan, S., Corke, T. C., and He, C., "Plasma Actuators for Hingeless Aerodynamic Control of an Unmanned Air Vehicle," AIAA Paper 2006-3495, June 2006.

[2] Corke, T. C., Cavalieri, D., and Matlis, E., "Boundary Layer Instability on a Sharp Cone at Mach 3.5 with Controlled Input," *AIAA Journal*, Vol. 40, No. 5, 2002, pp. 1015–1018.

[3] Roth, J. R., Sherman, D. M., and Wilkinson, S. R., "Electrohydrodynamic Flow Control with a Glow-Discharge Surface Plasma," *AIAA Journal*, Vol. 38, No. 7, 2000, pp. 1166–1172.

[4] Corke, T., Jumper, E., Post, M., Orlov, D., and McLaughlin, T., "Application of Weakly Ionized Plasmas as Wing Flow Control Devices," AIAA Paper 2002-0350, Jan. 2002.

[5] Post, M. L., and Corke, T. C., "Separation Control on High Angle of Attack Airfoil Using Plasma Actuators," *AIAA Journal*, Vol. 42, No. 11, 2004, pp. 2177–2184; also AIAA Paper 2003-1024, Jan. 2003.

[6] Post, M. L., and Corke, T., "Separation Control Using Plasma Actuators: Stationary & Oscillating Airfoils," AIAA Paper 2004-0841, Jan. 2004.

[7] Corke, T. C., He, C., and Patel, M. P., "Plasma Flaps and Slats: An Application of Weakly-Ionized Plasma Actuators," *AIAA Journal* (to be published); also AIAA Paper 2004-2127, 2004.

[8] Jacob, J., Rivir, R., Campbell, C., and Estevedoreal, J., "Boundary Layer Flow Control Using AC Discharge Plasma Actuators," AIAA Paper 2004-2128, June 2004.

[9] Patel, M. P., Sowle, Z. H., Corke, T. C., and He, C., "Autonomous Sensing and Control of Wing Stall Using a Smart Plasma Slat," AIAA Paper 2006-1207, Jan. 2006.

[10] Corke, T. C., Mertz, B., and Patel, M. P., "Plasma Flow Control Optimized Airfoil," AIAA Paper 2006-1208, Jan. 2006.

[11] Enloe, L., McLaughlin, T., VanDyken, R., Kachner, Jumper, E., and Corke, T. C., "Mechanisms and Response of a Single Dielectric Barrier Plasma Actuator: Plasma Morphology," *AIAA Journal*, Vol. 42, No. 3, 2004, pp. 589–594.

[12] Enloe, L., McLaughlin, T., VanDyken, R., Kachner, Jumper, E., Corke, T. C., Post, M., and Haddad., O., "Mechanisms and Response of a Single Dielectric Barrier Plasma Actuator: Geometric Effects," *AIAA Journal*, Vol. 42, No. 3, 2004, pp. 595–604.

[13] Corke, T. C., and Post, M., "Overview of Plasma Flow Control: Concepts, Optimization, and Applications," AIAA Paper 2005-0563, Jan. 2005.

[14] Patel, M. P., Ng, T. T., Vasudevan, S., Corke, T. C., Post, M. L., McLaughlin, T. E., and Suchomel, C. F., "Scaling Effects of an Aerodynamic Plasma Actuator," AIAA Paper 2007-0635, Jan. 2007.